International Journal of GEOMATE, Jan., 2025 Vol.28, Issue 125, pp.27-35
ISSN: 2186-2982 (P), 2186-2990 (O), Japan, DOI: https://doi.org/10.21660/2024.124.4547
Geotechnique, Construction Materials and Environment

SUBSIDENCE OF THE FOUNDATION GROUND PREVIOUSLY INDUCED INTERNAL EROSION

*Mari Sato[1] and Tatsuki Mihara[2]

[1]Academic Assembly Institute of Environmental Systems Science, Shimane University, Japan;
[2]Faculty of Life and Environmental Sciences, Shimane University, Japan

*Corresponding Author, Received: 07 May 2024, Revised: 22 Sep. 2024, Accepted: 15 Nov. 2024

ABSTRACT: Levees and the beneath foundation ground sometimes cause consolidation settlements. When the consolidation estimation is underestimated in advance, the structures and residents are damaged by consolidation. In addition, levees are subjected to piping and boiling with heavy rainfalls, which often have coarse permeable layers. The seepage is concentrated through coarse permeable layers. Owing to the repetition of regular rainfall and the changes in water levels, internal erosion occurs between a permeable and a finer soil layer. This study aims to reveal the effect of internal erosion on consolidation. Clay, including granular soil, is used to simulate both internal erosion and consolidation. First, long-term seepage is imposed on a soil specimen with a coarse layer. Then, clayey soil samples are obtained from the specimen subjected to seepage, and a consolidation test is conducted. The soil properties related to consolidation are revealed in several experimental cases. A numerical analysis is conducted using the experimentally obtained parameters to simulate the consolidation for embankment construction. Finally, the influence of internal erosion on consolidation is discussed. The soil consolidation behavior is similar to that of the clayey material when the specimen is loosely compacted. However, the behavior of the dense material appears to be sandy; consolidation is rapidly completed. The loosening caused by internal erosion is dissipated, and the consolidation properties approach those of the soil sample with a similar initial compaction degree. Finally, a practical application method for the internal erosion effect is proposed.

Keywords: Consolidation, Subsidence, Internal erosion, Contact erosion, Seepage

1. INTRODUCTION

Consolidation settlement sometimes occurs, particularly in soft clay layers. When the low permeable soil is loaded, drainage is slow, and excess pore water pressure is generated. The soil is settled and compressed slowly with the dissipation of the pore water pressure. Well-known consolidation layers include, for example, marine clay [1,2] and alluvial clay [3]. Levees are sometimes consolidated through structural construction, and appropriate prevention methods have been discussed [4,5]. The settlement of levees after their application induces damage not only to the levee itself but also to neighboring structures and residents. A previous study [6] reported that levee settlement may lead to greater liquefaction damage. An analytical method for consolidation was also developed [7, 8]. When the estimation of consolidation is underestimated, additional repairs and construction should be performed.

By contrast, contact erosion between coarser and finer soils often occurs in the vicinity of levees [9]. Seepage is concentrated through the coarser soil layer, and a fraction in a finer soil layer is eroded to a surrounding coarser layer. The details of these phenomena were simulated using numerical analysis [10]. In addition, the coarser soil layers of levees sometimes cause piping or boiling under heavy rainfall [11]; experiments and numerical analyses were conducted [12,13] to reveal the boiling mechanism of sand layers in the vicinity of dikes. The boiling mechanism caused by the cofferdams is also studied [14].

The internal erosion and structural evolution of soil–rock mixtures have been studied [15], and the location of the soil–rock mixture obviously influenced the structural change of the mixture. This study aims to determine the influence of internal erosion on consolidation settlement. Internal erosion may change both density and soil structure. After the foundation ground is slightly eroded by infiltration, the consolidation behavior may change from that of the ground without erosion. A clayey material containing coarse grains was used to simulate both internal erosion and consolidation. This study conducted a consolidation test for soil samples subjected to long-term seepage, allowing internal erosion to the coarser soil. The consolidation parameters of the soil subjected to erosion were obtained and applied to a numerical analysis simulating practical sites.

2. RESEARCH SIGNIFICANCE

This study contributes to the design of the levees and embankments. Settlement is previously simulated, but sometimes, the calculated values do not correspond to the practical sites. This study reveals the influence of internal erosion on settlement, and a

more precise design for settlement can be achieved. When the embankment is internally eroded for a long time, the embankment may settle more largely. This study finally proposed the m_v estimation method for soil-induced internal erosion.

3. CONSOLIDATION TEST

3.1 Test Material

Two materials were used to simulate the erosion between a fine soil layer and a coarse soil layer. The main material was the fine soil that was used to evaluate subsidence following suffusion. Kaolin clay, called clayey soil hereafter, was used for the fine soil, which is the original soil containing not only finer fractions but also coarser fractions. In this study, both internal erosion and consolidation were simulated, and the original kaolin soil, including non-swelling clay, was applied. The particle size distribution is shown in Fig. 1. Clayey soil contained approximately 60 % of finer fractions measuring less than 0.075 mm, and the average grain size, d_{50}, was 0.02 mm. Other properties were as follows: soil particle density ρ_s was 2.463 g/cm^3, maximum dry density ρ_{dmax} was 1.493 g/cm^3, and the optimum water content w_{opt} was 24.2%.

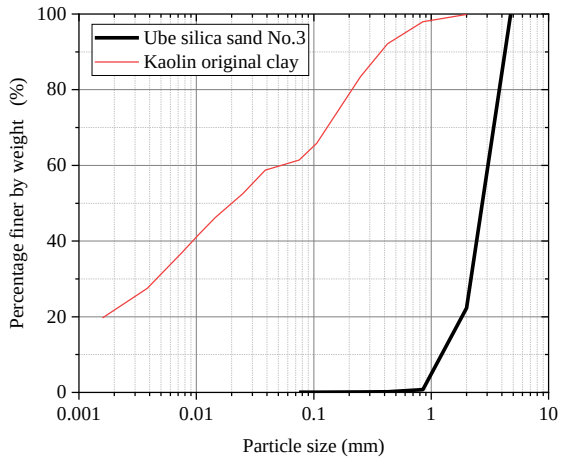

Fig. 1 Particle size distribution

Ube silica sand no. 3 was used for the coarse soil, the grain size distribution of which is shown in Fig. 1; D_{50} was 2.72 mm. Terzaghi's rule determined that $D_{15}/d_{85} < 4$ was necessary to prevent internal erosion, where D_{15} indicates 15% particle size of the coarser material and d_{85} indicates 85% particle size of the finer material. For the two tested materials, D_{15}/d_{85} was 5.25. In addition, based on the US Army general design for earth and rockfill dams [16], the base soil is categorized as No. 2; D_{15} of the filter soil should be less than 0.7 mm. However, D_{15} of the coarse soil in the experiments was 1.50 mm. Therefore, the tested materials did not satisfy the general standards, which suggested that an evident collapse owing to large amount of erosion did not occur; however, the materials were under threat by small-scale internal erosion.

3.2 Test Apparatus and Procedure

A flowchart of the procedure is shown in Fig. 2. Two processes, seepage and erosion, and consolidation, were combined. First, the clayey soil was compacted into a mold under the determined initial density and optimum water content. The test apparatus was the same as that used in the constant head permeability test, with reference to JIS A 1218 [17]. The mold was 10 cm in diameter and 12.7 cm in height. The bottom plate had small holes, and a metal mesh plate was placed on it. The clayey soil was compacted into five layers with a thickness of 2 cm and a total thickness of 10 cm. The remaining space was filled with coarse soil. After the mold was filled, the specimen was submerged and connected to a decompression device for saturation.

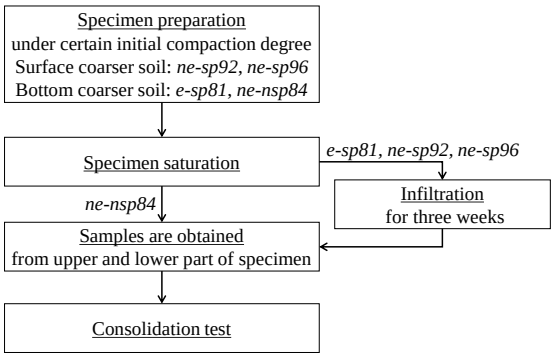

Fig. 2 Flowchart of series of experiments

Following saturation, the specimens were infiltrated for three weeks, as shown in Fig. 3, except for e-nsp84. The soil layers of the specimens shown in the figure correspond to e-sp81 and e-nsp84. The details of the experimental cases are described subsequently. e-nsp84 consolidated after saturation.

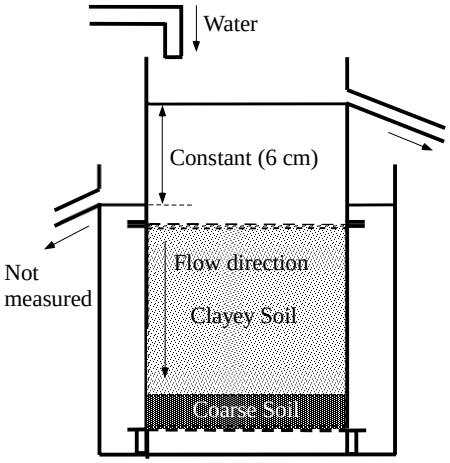

Fig. 3 Schematic illustration of infiltration test for e-sp81

Filtration was in the downward direction, and the head loss from the inlet to the outlet was 6 cm. During infiltration, the clayey soil was eroded under e-sp81 because the coarse soil was placed at the bottom. However, the amount of the eroded soil was not measured in this study.

The consolidation process was based on one-dimensional consolidation properties using incremental loading (JIS A 1217 [17]). The clayey soil samples for the consolidation test were obtained using a cutter ring. Two samples, i.e., the upper and lower portions of the specimen in the mold, were pulled out. Note that the low-density specimens, e-sp81 and e-nsp84, were extremely soft after removing the mold and were filled into the consolidation mold after it was set up. The soil samples were consolidated in eight steps, as described in JIS A 1217. Each step required one day. The displacement was automatically recorded using digital indicators throughout the test, and the measured displacement at the elapsed time determined by JIS A 1217 was obtained. The other test procedures were similar to those of JIS A 1217, by which the soil coefficients related to consolidation were calculated.

Finally, a finer fraction of soil samples under 0.075 mm was measured by sieving to reveal the suffusion degree.

3.3 Test Conditions

Four test cases were considered: e-sp81, e-nsp84, ne-sp92, and ne-sp96 (Table 1). The consolidation process was similar in every case.

Table 1. Experimental cases

Case	e-sp81	e-nsp84	ne-sp92	ne-sp96
coarse soil	bottom	bottom	surface	surface
infiltration	3 weeks	no	3 weeks	3 weeks
D_c (%)	81	84	92	96

The initial average compaction densities of the two samples were separated into lower- and higher-density cases; the lower densities were e-sp81 and e-nsp84, and the higher densities were ne-sp92 and ne-sp96. The end of each case name represents the compaction degree D_c (%) of the soil at the beginning of the consolidation, calculated from the void ratio and soil particle density.

Because the coarse soil located below the clayey soil imposed downward seepage, e-sp81 of the clayey soil is erodible. Although the location and thickness of the two soils were the same as those of e-sp81, seepage was not imposed on e-nsp84; the case had a low density, and prevention from disturbance with long-term penetration was difficult. The coarse soil was placed above the clayey soil for two high-density cases, i.e., ne-sp92 and ne-sp96, that adequately simulated compacted ground that sometimes imposed seepage without erosion.

3.4 Test Results

All the results presented here are the average values of the upper and lower portions of the specimen. The two portions exhibited similar trends in general; the void ratio difference among the portions was less than 10 % for all cases. Certain differences between the two portions are not discussed in this paper. Taylor's square root of time fitting method was applied.

2.4.1 Compression curve

The compression curve for each case is shown in Fig. 4. The consolidation pressures, p, of the eight loading stages were 9.8, 19.6, 39.2, 78.5, 157, 314, 628, and 1256 (kN/m^2). The void ratio was proportional to the initial degree of compaction of the sample; e-sp81 had the largest void ratio, whereas ne-

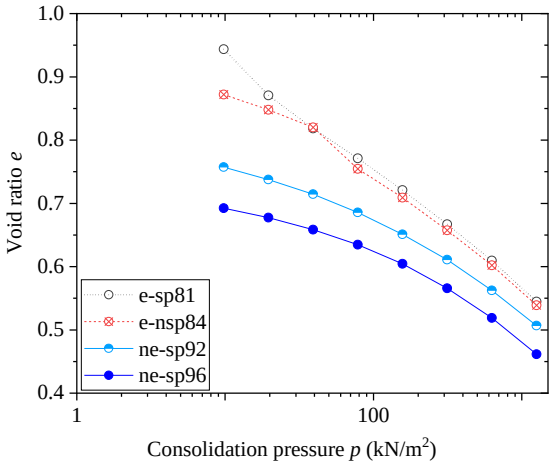

Fig. 4 Compression curves

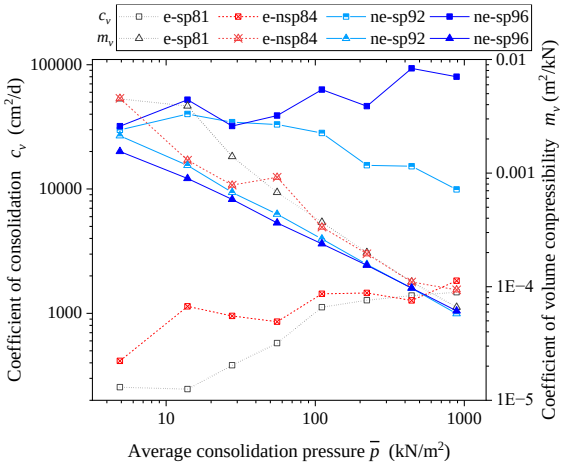

Fig. 5 Coefficient of consolidation, c_v, and coefficient of volume compressibility, m_v

Table 2. Fine fraction content after consolidation

Case	Fine fraction content, F_c (%)
original	61.4
e-sp81	60.5
e-nsp84	58.3
ne-sp92	56.9
ne-sp96	56.4

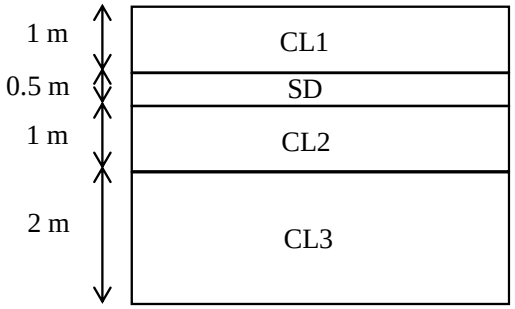

Fig. 7 Components of the foundation ground

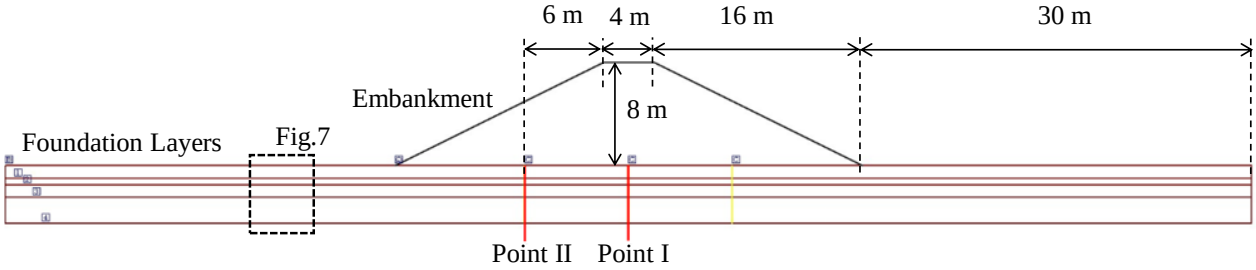

Fig. 6 Embankment model for analysis

sp96 had the smallest. This tendency did not change with an increase in the loadings. The consolidation yield stress was insignificant in these experiments. The past pressure owing to the overburden pressure and hydraulic pressure on the clayey soil was inferred to be negligible and estimated to be less than 5 kN/m^2; over-consolidation might not have occurred. The line shape was a gentle curve for all cases, except for e-sp81 that had a straight line through the loading. The lines of e-sp81 and e-nsp84 overlapped in the range of loading steps exceeding 39.2 kN/m^2.

2.4.2 Coefficient of consolidation and coefficient of volume compressibility

The coefficient of consolidation, c_v (cm^2/day), and coefficient of volume compressibility, m_v (m^2/kN), are shown in Fig. 5. The average consolidation pressure, $\bar{p}$ (kN/m^2), was calculated using Eq. (1).

$$\bar{p} = \sqrt{p \cdot p'} \quad (1)$$

where $\boldsymbol{p'}$ (kN/m^2) denotes the consolidation pressure of the former stage of loadings.

The coefficient of consolidation, c_v, was classified into two groups: high (ne-sp92 and ne-sp96) and low (e-sp81 and e-nsp84) initial densities. High-density samples had higher values than typical alluvial clays [14]. Except for ne-sp92, the coefficient of consolidation gradually increased with the increase in the loading pressure.

Coefficient of volume compressibility, m_v, was inversely related to the initial density; the dense and loose samples indicated low and high values of m_v, respectively. In addition, the coefficient value decreased with an increase in the load. The mechanisms underlying these phenomena are discussed below.

A comparison of e-sp81 and e-nsp84, with and without erosion, showed clear differences in the range of small loadings (less than 55.5 kN/m^2). This trend was similar to that of the compression curves.

2.4.3 Finer fraction

The finer fractions of the samples after consolidation are listed in Table 2, along with the original value of the clayey soil. The finer fraction was similar for all the cases, including that of the original soil. As an evident decline in the finer fraction was not observed in all the cases, suffusion that the finer fraction of the clayey soil eroded through the pores of its coarser fraction rarely occurred or was not observed. However, to completely prevent the clayey soil from erosion from the contact plane of the coarse soil is difficult, as mentioned previously. The experiments did not directly verify the occurrence of erosion; however, e-sp81 had a lower density than that of e-nsp84. The clayey soil was suggested to be eroded to the coarse soil and generally loosened owing to long-term seepage.

4. CONSOLIDATION ANALYSIS

A two-dimensional consolidation analysis was performed using a river dike model, although the model does not simulate specific on-site dikes. Soil parameters, i.e., c_v, m_v, e-log$P$ and unit weight were obtained from above mentioned experiments. The software named “Calculation of consolidation settlement Ver.11” by FORUM8 was applied. The

software performs calculation based on the one-dimensional Terzaghi's consolidation theory applied to various design standards. Although the precise on-site conditions were not simulated, the consolidation of the embankment was calculated using a common method.

3.1 Conditions of Embankment Model

3.1.1 Overview of simulated dike model

The general embankment model is shown in Fig. 6 with reference to hazard reports and previous studies [12, 18]. The consolidation settlement was calculated for the foundation layers by the construction of the dike. The dike was 8 m high, and the crown was 4 m wide. The slope on both sides was 1:2. The unit weight of the dike was a typical value of 18.0 kN/m^3 and required 27 days to be constructed to the aforementioned height (30 cm constructed per day).

Table 3. List of analytical cases

Case	EL-92	NEL-92	NED-92
CL1	e-sp81	e-nsp84	ne-sp92
CL2	e-sp81	e-nsp84	ne-sp92
CL3	ne-sp92	ne-sp92	ne-sp92
Case	EL-96	NEL-96	NED-96
CL1	e-sp81	e-nsp84	ne-sp96
CL2	e-sp81	e-nsp84	ne-sp96
CL3	ne-sp96	ne-sp96	ne-sp96

The 30 m length of the foundation layers from the toes of the dike was simulated. The foundation ground consisted of four layers: three clayey layers and one coarse soil layer. The layers of the foundation ground are shown in Fig. 7. The layers, from the surface, are named CL1, SD, CL2, and CL3. CL indicates a clayey soil layer, and SD indicates a coarse soil (sand) layer. The total thickness was 4.5 m and each layer thickness was 1.0, 0.5, 1.0, and 2.0 m, respectively. CL1 and CL2 were respectively placed above and below SD, which had the same properties and were simulated to be erodible from the contact of the coarse soil layer. CL3 was not erodible and was located far from the coarse soil layer. Details of the analytical method and conditions are described later. Finally, the total ultimate settlement, including the immediate settlement of SD, was calculated at two points: Point I and Point II of the foundation layers along the vertical direction. The horizontal location of Point I was at the center of the embankment crown, and that of Point II was on the upward side of the slope, 10 m from the toe. None of the trends changed between the two points. This paper introduces the details of the results for Point I.

3.1.2 Details of analytical cases

Table 3 lists the inputs applied to the experimental cases shown in Table 1 for each layer. Six foundation ground conditions were simulated using a combination of CL1 (CL2) and CL3, as listed in the table. Every layer allowed for drainage from both the upper and lower sides. Only primary consolidation was simulated, and the settlement was calculated by the change of void ratio, Δe, or coefficient of volume compressibility, m_v. The internal stress in the ground was calculated using the Boussinesq's equation. SD was the same in all the cases, and immediate settlement was calculated using the relationships between the void ratio (N = 10-30) and pressure established by Hough [19].

For EL-92, NEL-92, and NED-92, the consolidation parameters of ne-sp92 were applied for CL3. The input parameters were c_v, m_v, and the compression e-log$P$ curve through loadings for each case. EL-92 simulated the clayey soil layers (CL1 and CL2) in the vicinity of the coarse soil layer (SD), that were eroded and loosened. NEL-92 also had loosened clayey soil layers; however, the analytical parameters of e-nsp84 were used as inputs. Therefore, ground loosening was considered but not the influence of erosion. NED-92, that had the same clayey soil layers applying ne-sp92 results, was a healthy structure without erosion or loosening. EL-96, NEL-96, and NED-96 are under the similar situation as EL-92, NEL-92, and NED-92, respectively; however, the parameters of ne-sp96 were input for non-eroded soil (see Table 3). Water level reached to the ground surface, and submerged unit weight was used. The layer input parameters of e-sp81, e-nsp84, ne-sp92, ne-sp96 and the sand layer were 7.1, 7.3, 8.0, 8.4, and 10.0 (kN/m^3), respectively.

3.1.3 Analytical results

Ultimate settlement at Point I of entire layers and each layer for all cases are represented in Fig. 8 and Fig. 9 calculated from Δe and m_v, respectively. The overall tendency was equivalent to that at Point II, inducing a smaller settlement for a smaller surcharge. The settlement of SD was similar in all cases and negligibly small, approximately 0.01 m. General trend was the same between the settlement calculated from Δe and m_v, although the estimation from m_v was larger. The entire tendency relied on CL1 settlement because a small overburden pressure before consolidation maintained a large initial void ratio. The settlements of the other layers were similar in all cases. Irrespective of the initial density of CL3, the cases with eroded layers, such as EL-92 and EL-96, induced a large settlement. When the foundation consisted of only a healthy layer, such as in NED-92

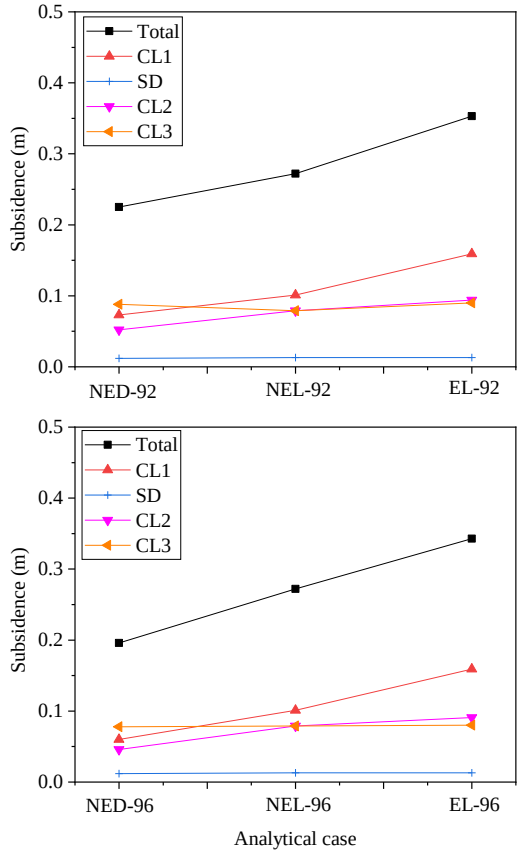

Fig. 8 Ultimate subsidence calculated from void ratio

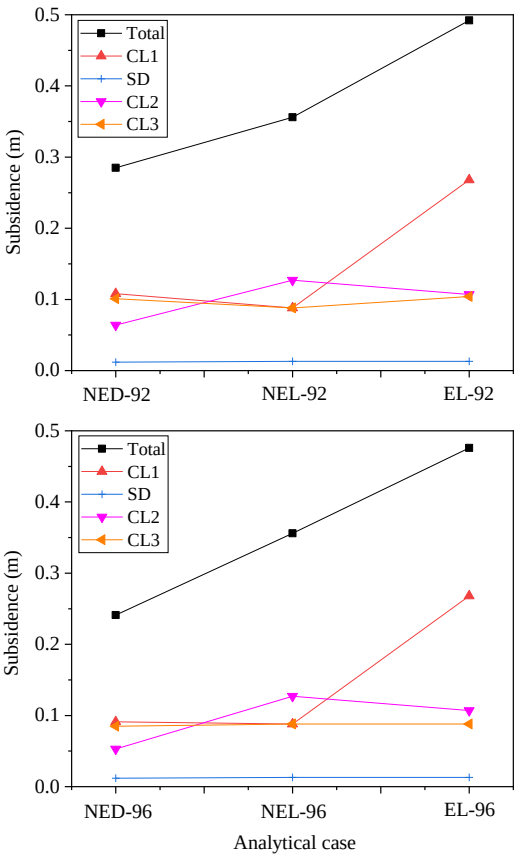

Fig. 9 Ultimate subsidence calculated from m_v

and NED-96, the settlement was small. Compared with EL-92 and NEL-92 (or EL-96 and NEL-96), the settlement was clearly enlarged by the internal erosion evaluation for the analysis. Details of this process are discussed in the following chapter. However, the amount of ultimate subsidence was limited, and consolidation was accomplished in a short period for all cases; the number of days to reach the degree of consolidation U = 90 % was within 27 days of construction. The numerical analysis using the examined clayey soil did not simulate the practical ground, particularly in terms of the consolidation speed. In the future, the testing material should be changed to simulate onsite consolidation.

5. DISCUSSIONS

4.1 Subsidence Mechanism

Consolidation and internal erosion are regarded as two different phenomena and treated separately in most previous studies. In particular, consolidation was evaluated for clayey soil and internal erosion was done for sandy soil. Whereas official evaluation and prevention methods are required, they have not yet been devised. This study used a sand–clay mixed material and considered the effect of subsidence due to internal erosion. Consequently, the common time-delayed consolidation process was not evident; however, an increase in subsidence was observed. The experimental results did not show the typical consolidation process, particularly for high-density samples such as ne-sp92 and ne-sp96. Because the material consisted of both finer and coarser fractions, the internal friction worked through the soil skeleton of larger particles with dense samples, and compression was effectively caused by the changes in the soil skeleton. The details of inside the samples were not investigated in this study. However, previous studies (e.g., Guo and Zhao [20]) have suggested that stress chains of granular materials develop with compression.

Internal erosion can affect consolidation when the grain size distribution is changed. In this study, the grain size distribution did not change, whereas the consolidation behavior varied. The estimated mechanism is the reconstruction of the soil skeleton. The initial soil skeleton was dynamically stable when the specimen was subjected to a compaction force. After seepage was imposed and the soil particles were eroded, the soil skeleton was reconstructed to be stable against the seepage force, which was not necessarily dynamically stable. The soil was loosened by the loss of soil particles by internal erosion. The chains of the coarser fractions did not work adequately, and the finer fraction determined the subsidence process in the low-density samples. Internal erosion caused a tendency change from the immediate settlement of sand to the consolidation of

clayey soil for the sand–clay mixed materials. The coefficient of consolidation, c_v, was significantly larger for the high-density samples and the compression speed was higher than those of common clay materials. When the material density decreased, the coefficient of consolidation was close to that of the typical clay. In the pilot study, the same material was used and the total load of the same embankment was momentarily subjected, suggesting that the consolidation speed was different between the loose and dense conditions. The speed was lower for the loose materials than for dense materials. This trend was also implied by the hydraulic conductivity estimated from the consolidation test. The hydraulic conductivity of the loose samples was approximately one-tenth that of the high-density samples; this was not directly measured but was calculated based on Terzaghi's consolidation theory and experimental results. This trend indicated that the tested soil compression behavior was more similar to that of typical clay consolidation when the soil was loosely compacted.

4.2 Application for the Practical Ground

4.2.1 Discussion of numerical analysis

The increase ratio of ultimate subsidence was defined as the ratio of the total consolidation to that of NED-96, and the ratio of NED-96 was defined as 1.0. Fig. 10 shows the increase ratio calculated from m_v in the ascending order. As shown in the figure, ground loosening induced an increase in consolidation. In addition, the settlement was twice that of the densest soil when the influence of internal erosion was considered. If the ground was internally eroded after the ground survey, consolidation was underestimated, and further consolidation might occur. For example, the densities of the foundation layers and dikes were surveyed when the dike was constructed. The inside soil had been eroded for a long time, the soil layers loosened, and the actual consolidation subsidence might exceed the initially designed consolidation subsidence.

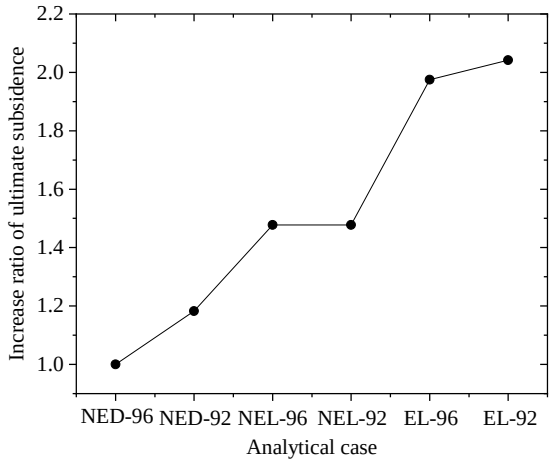

Fig. 10 Increase ratio in subsidence owing to low density and internal erosion

4.2.2 e–m_v relationships

The relationship between void ratio e and coefficient of volume compressibility m_v is summarized in Fig. 11. Void ratio e at an average pressure $\bar{p}$ for each loading was visually estimated

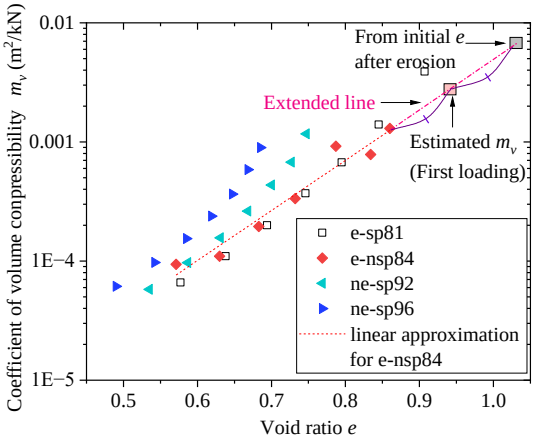

Fig. 11 e–m_v relationships and m_v estimation method

from the compression curves shown in Fig. 4. As shown in Fig. 11, the coefficient of volume compressibility was large for highly compacted samples. The soil contains granular materials that become dense by compression. Then, the soil is hard to be deformed and m_v is decreased by the increase in loads. However, the lines of e-sp81 and e-nsp84 were approximately similar; this is also suggested by the compression curves. The loosening caused by internal erosion could differ from that caused by a lack of initial compaction. The loosening owing to internal erosion rapidly disappeared with an increase in the load, and the line of the eroded sample was close to that of the non-eroded sample with a similar initial compaction degree. One reason for this phenomenon was that seepage and loading were in the same vertical direction. The details of this mechanism will be studied in the future. The coefficient of volume compressibility for eroded soil can be estimated from e–m_v relationships for soil without erosion. When the void ratio increased with erosion and the increased void ratio could be estimated, m_v could be estimated from the extended approximate line of e–m_v relationships calculated from the soil without erosion. In Fig. 11, the linear approximation using the least-squares method is depicted for e-nsp84. By extending the line to a certain void ratio of the ground-imposed internal erosion, m_v could be estimated; m_v is useful for calculating consolidation. For example, experiments showed that m_v was clearly different for the first load between with and without erosion; this should be estimated to determine the influence of erosion. For the other loading steps, m_v value for non-eroded soil can be used for eroded soil. A simple estimation method was proposed as follows: First, the

line was extended to the void ratio after erosion. The estimated m_v of the eroded soil for the first loading was somewhere on the extended line. Then, the midpoint of the extended line was estimated m_v, that did not differ significantly from the measured value of the experiments. This midpoint was selected for this study because the void ratio decreased gradually as loading progressed. An appropriate approximation method and the points on the line should be discussed in the future study. Although the difference clearly appeared only at the first loading step in the experiments, future studies should confirm that this trend is common, irrespective of the soil and loading conditions.

6. CONCLUSION

This study evaluated the influence of internal erosion on settlement, and the following conclusions were obtained:

1. The consolidation test revealed that the soil parameters varied with the initial density and loosening by internal erosion. The examined material contained a coarser fraction that led to complex behaviors. The behavior of dense samples was similar to that of sand; coefficient of consolidation c_v was large, and consolidation was quickly accomplished. By contrast, the loose samples were consolidated similar to clayey materials. The parameters of the eroded samples differed from those of the non-eroded samples at small loads.
2. A numerical analysis of embankment construction was performed for an on-site scale ground with multiple foundation layers. The analysis suggested that the necessity of including the influence of internal erosion; the loosened ground caused by internal erosion was largely consolidated.
3. The loosening caused by internal erosion could disappear when the loading was increased; this differed from the loosening caused by a lack of compaction. Loosening owing to compaction insufficiency remained even when a large loading was applied. However, a loosened soil structure caused by internal erosion could be reconstructed under large loads.
4. This study proposed an m_v consolidation estimation method for loosened ground caused by internal erosion. The experimental results suggested that the consolidation properties of the eroded low-density soil approached the values of the same soil without erosion through consolidation, with a similar initial compaction degree with an increase in the load. If the void ratio after erosion was estimated, m_v could be simulated.
5. Additional experiments using different materials and conditions are required to reveal the entire influence of internal erosion on subsidence. The erodible zones in the finer soil surrounding the sandy layers should be discussed. Additionally, the tested material consolidated much faster than common clay did in the simulation. The approximate line for e–m_v relationship was depicted as a straight line in this study. Applications to over-consolidated materials and more profitable line forms should be discussed in the future. The number of experimental cases was limited; common trends and mechanisms should be verified further.
6. Ministry of Land, Infrastructure, Transport, and Tourism in Japan stipulated that subsidence should be calculated for river dikes comprising soft ground. A filter criterion was established to prevent erosion. When loosening or disturbed areas are observed during periodic inspection, re-evaluation of consolidation subsidence is recommended. Additionally, when soil layers are permeable and internal erosion can easily occur, the risks of internal erosion and underestimating consolidation should be considered in advance.

7. ACKNOWLEDGMENTS

Mr. Nagae, an alumnus of Shimane University, cooperated in conducting the experiments and summarizing the results obtained in this study.

This study is financially supported by the River Fund of The River Foundation, Japan, and JSPS KAKENHI, Grant number 22K04312. We would like to thank Editage [http://www.editage.com] for editing and reviewing this manuscript for English language. The authors thank the Faculty of Life and Environmental Sciences at Shimane University for the financial support in publishing this report.

8. REFERENCES

[1] Bjerrum L., Engineering Geology of Norwegian Normally-Consolidated Marine Clays as Related to Settlements of Buildings, Géotechnique, Vol. 17, Issue 2, 1967, pp.83-118.

[2] Watabe Y., Udaka K. and Morikawa Y., Strain Rate Effect on Long-term Consolidation of Osaka Bay Clay, Soils and Foundations, Vol. 48, No. 4, 2008, pp.495-509.

[3] Fujiwara H., Yamanouchi T., Yasuhara K. and Ue S., Consolidation of Alluvial Clay Under Repeated Loading, Soils and Foundations, Vol. 25, No. 3, 1985, pp.19-30.

[4] Tsubota K., Nakajima K., and Nishigaki M., A Study of the Countermeasures for the Residential Ground Settlement by the Embankment in Soft Gound, Japanese Journal of JSCE, Vol. 63, No. 3, 2007, pp.323-334.

[5] Nguyen, N.T., Controlling the Settlement of the

Low Embankment on Soft Ground by Surcharge Preloading Method, International Journal of GEOMATE, Vol. 25, Issue 108, 2023, pp.1-10.
[6] Okamura M., Tamamura S. and Yamamoto R., Seismic Stability of Embankments Subjected to Pre-deformation due to Foundation Consolidation, Vol. 53, No. 1, 2013, pp.11-22.
[7] Manoharan N. and Dasgupta S.P., Consolidation Analysis of Elasto-plastic Soil, Computer & Structures, Vol. 54, No. 6, 1995, pp.1005-1021.
[8] Zhang, Y., Zong, M., Wu, W., Zong, Z., Mei, G. and Wang, C., One-dimensional Consolidation Analysis of Layered soil with Exponential Flow under Continuous Drainage Boundary, Numerical and Analytical Methods in Geomechanics, 2024, pp.1-16.
[9] Bonelli S., Ed., Erosion in Geomechanics Applied to Dams and Levees, ISTE Ltd and John Wiley & Sons, Inc., 2013, pp. 1-388.
[10] Chang L. and Chen Q., Simulation on the Process of Contact Erosion between Cohesionless Soils, KSCE Journal of Civil Engineering, Vol. 25, No. 8, 2021, pp.2884-2892.
[11] Sato H., Nakayama O. and Sako S., A Case Investigation on Leakage at Tone River Dike, Advances in River Engineering, JSCE, Vol. 11, 2005, pp.83-86.
[12] Sato M., Sakamoto N., Piping Risks Because of Internal Erosion to an Embankment Having a Permeable Foundation Layer, Ground Engineering, Vol. 40, No. 1, 2022, pp.89-99.
[13] Rajabi A.M., Langroudi S.G., Zad A. and Langroudi M.G., Numerical and Laboratory Investigation of Boiling Various Sandy Soils at Downstream of Hydraulic Levees, Arabian Journal of Geosciences, Vol. 16, 2023, article number 583.
[14] Matsuda, T., Naito, N. and Miura, K., Model Tests on Sand Boiling around Cofferdam Considering the Effect of Geomaterial Properties, International Journal of GEOMATE, Vol. 24, Issue 102, 2023, pp.50-57.
[15] Mao X., Cai P., Fu J. and Dai Z., Study on Internal Erosion and Structural Evolution Mechanism of Soil-Rock Mixture, Natural Hazards, Vol. 118, 2023, pp.1739-1764.
[16] US Army Corps of Engineers, Appendix B in General Design and Construction Considerations for Earth and Rock-Fill Dams, 2004, pp. 1-8.
[17] Japanese Geotechnical Society, Japanese Geotechnical Society Standards: Laboratory Testing Standards of Geomaterial, Vol. 1, Maruzen co. ltd, 2015, pp.1-262.
[18] Japanese Geotechnical Society, Investigation of River Dikes, from Examination to Maintenance, Maruzen Co. ltd, 2020, pp.1-149.
[19] Hough B.K., Basic Soils Engineering, The Ronald Press, 1957, pp.109.
[20] Guo N. and Zhao J., The Signature of Shear-Induced Anisotropy in Granular Media, Computers and Geotechnics, Vol. 47, 2013, pp.1-15.